Eksakta : Berkala Ilmiah Bidang MIPA
VOLUME 27 NO 06 2026, pp 1194-1214
ISSN : Print 1411-3724 — Online 2549-7464
DOI : https://doi.org/10.24036/eksakta/vol27-iss06/780

Eksakta
Berkala Ilmiah Bidang MIPA
http://www.eksakta.ppj.unp.ac.id/index.php/eksakta

Article

Stability and Sensitivity Analysis of a Langkap–Forage Vegetation–Javan Rhinoceros Model under Langkap Control and Human Pressure

Article Info

Article history :
Received October 15, 2026
Revised November 17, 2026
Accepted November 23, 2026
Published December 30, 2026
In Press

Keywords :
Sensitivity analysis,
Javan rhinoceros,
local stability,
Langkap,
mathematical model

Siti Dwi Nuraini[1], Rudianto Artiono[2*]

[1]Department of Mathematics, Faculty of Mathematics and Natural Science, Universitas Negeri Surabaya, Surabaya, Indonesia

Abstract. The persistence of the Javan rhinoceros (*Rhinoceros sondaicus*) in Ujung Kulon National Park is linked to forage availability, which may be affected by Langkap (*Arenga obtusifolia*). This study develops a three-dimensional ordinary differential equation model of interactions among Langkap (L), forage vegetation (P), and the Javan rhinoceros population (R), incorporating Langkap control and human pressure. The analysis addresses positivity and boundedness, equilibrium points, local stability, numerical simulations, and normalized parameter sensitivity. Eight equilibrium points are identified, including one biologically meaningful interior equilibrium, $(E_7) = 142.857, 77.375, 96.736)$, which is locally asymptotically stable because all Jacobian eigenvalues have negative real parts. Simulations from four initial conditions converge toward (E_7). Sensitivity analysis shows that the Langkap control parameter (u) most strongly affects L^*, whereas α has the greatest influence on P^*. For R^*, the mortality parameter (μ) has the largest absolute normalized sensitivity, followed by a; H and β have equal effects. A positive Langkap equilibrium requires $u < r_L$. This condition provides a theoretical reference for Langkap control, not an operational recommendation without field-data calibration. The results characterize qualitative model dynamics rather than actual population estimates.

This is an open acces article under the CC-BY license.

This is an open access article distributed under the Creative Commons 4.0 Attribution License, which permits unrestricted use, distribution, and reproduction in any medium, provided the original work is properly cited. ©2026 by author.

Corresponding Author :
Rudianto Artiono
Department of Mathematics, Faculty of Mathematics and Natural Science,
Universitas Negeri Surabaya, Indonesia
Email : rudiantoartiono@unesa.ac.id

1. Introduction

The Javan rhinoceros (Rhinoceros sondaicus) is a critically endangered species whose remaining wild population is confined to Ujung Kulon National Park, Indonesia. Its long-term persistence depends on effective habitat protection and the availability of suitable food resources. A vegetation survey in the Javan Rhino Study and Conservation Area (JRSCA) recorded 241 plant species in the undeveloped area, including 89 species identified as rhinoceros food plants [1]. These findings demonstrate the importance of vegetation diversity in supporting the ecological requirements of the species. Therefore, maintaining suitable habitat and vegetation conditions remains an important component of Javan rhinoceros conservation and frontline management [2].

One vegetation-related concern in Ujung Kulon is the distribution of Langkap (Arenga obtusifolia), an invasive palm that may influence the availability of forage vegetation. Damarjati et al. [3] mapped the distribution of this species using PRISMA hyperspectral data and multiple endmember spectral mixture analysis (MESMA). Their study provides spatial information on Langkap occurrence but does not quantify its effects on forage availability or rhinoceros population dynamics. Research in other ecosystems has shown that changes in plant–herbivore interactions can influence vegetation structure and plant community dynamics [4]. Nevertheless, the relationship among Langkap abundance, forage vegetation, and the Javan rhinoceros requires further investigation within an integrated ecological framework.

Mathematical models provide a framework for examining interactions among plant resources, herbivores, and environmental limitations. Recent plant–herbivore models have investigated food limitation, population persistence, equilibrium behaviour, and stability [5-7]. Predator–prey studies have further examined nonlinear functional responses, bifurcation behaviour, and population dynamics under different ecological assumptions [8-10]. In particular, the Holling type II functional response has been applied in deterministic, stochastic, and discrete-time ecological models [9],[11-12].

In the present study, the Holling type II response represents the assumed saturation of forage consumption by the Javan rhinoceros. The carrying capacity of forage vegetation is assumed to decrease with increasing Langkap density, while human pressure is incorporated as a scenario factor that reduces the effective carrying capacity of the rhinoceros population. These relationships are introduced as phenomenological modelling assumptions rather than empirically established functions for Ujung Kulon. Sensitivity analysis is important for identifying parameters that influence ecological model outcomes and may require particular attention in management. In addition to parameter-based sensitivity analysis, structural sensitivity has also been investigated in ecological models.

Wyse et al. [13] examined structural sensitivity in predator–prey models with different functional responses, while Kuiper et al. [14] discussed the relationship between ecosystem stability and structural sensitivity in ecological models at equilibrium. Lusardi et al. [15] proposed biological criteria and Sobol analysis for comparing theoretical functional-response models, while Luján et al. [16] developed a protocol for conducting parameter sensitivity analysis in complex ecosystem models. Parameter uncertainty has also been examined in ecological models involving forest biomass and forest-dependent wildlife populations [17]. In invasive-species management, mathematical approaches have been used to investigate optimal resource allocation and control strategies [18-20]. Related studies have also examined the ecological effects of invasive species in harvested predator–prey systems [21] and optimal control strategies in plant–herbivore models [22]. Other studies have examined decisions concerning monitoring and control [23] and the integration of remote-sensing data into spatiotemporal management models [24].

Although these studies provide relevant approaches to ecological modelling and management, they address different species, ecological mechanisms, or analytical objectives. Field studies in Ujung Kulon have documented Langkap distribution, vegetation diversity, and the conservation context of the Javan rhinoceros [1-3]. Research on human pressure has also examined associations between human presence, environmental disturbance, and wildlife space use [25-26], while broader work has

reviewed carrying capacity in human–environment interactions [27]. However, an integrated dynamical model describing Langkap, forage vegetation, and the Javan rhinoceros while incorporating Langkap control and human pressure remains the focus of this study. Accordingly, this research formulates a three-dimensional ordinary differential equation model with state variables Langkap density (L), forage vegetation (P), and Javan rhinoceros population (R), and investigates solution positivity and boundedness, equilibrium points, local stability, numerical simulations, and normalized parameter sensitivity.

2. Research Methods

2.1. Research Approach

This study employs a mathematical modelling approach based on a three-dimensional system of ordinary differential equations describing the interactions among Langkap density (L), forage vegetation availability (P), and the Javan rhinoceros population (R). The research consists of several stages, including problem identification, literature review, mathematical model formulation, parameter determination, mathematical analysis, numerical simulation, and interpretation of the results. The overall research procedure is presented in Figure 1.

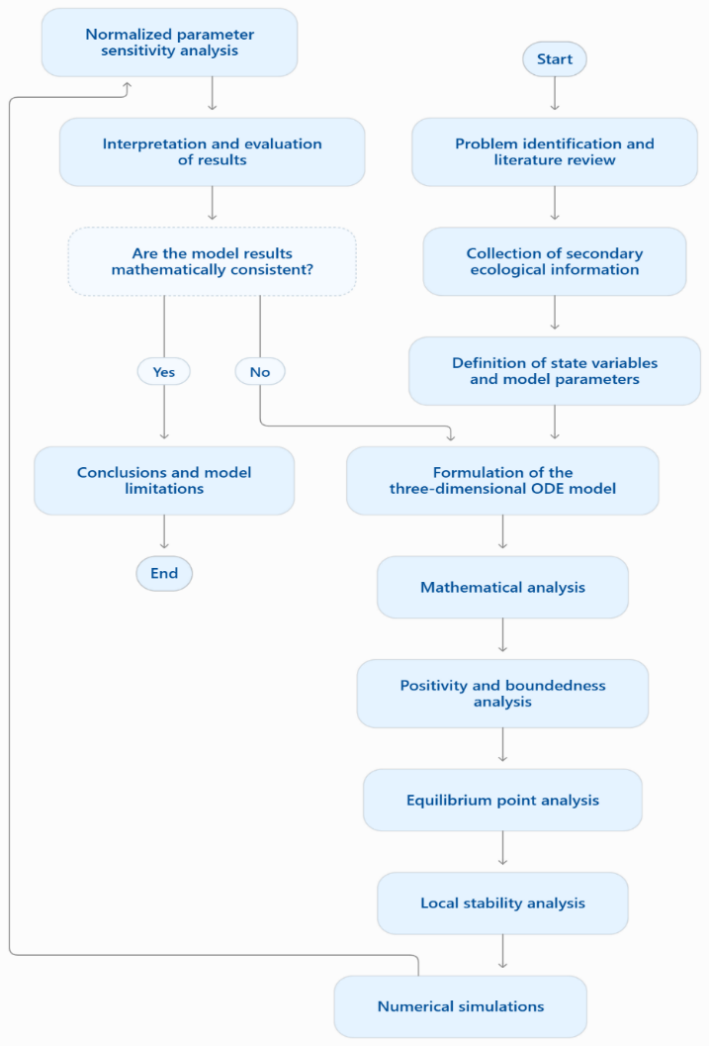


Figure 1. Schematic/Flowchart of research

The ecological information used to formulate the model is obtained from secondary sources, particularly published studies concerning Langkap distribution, vegetation diversity, and Javan rhinoceros conservation in Ujung Kulon National Park [1–3]. These studies provide the ecological context for defining the state variables and the assumed interaction mechanisms in the proposed model. The model parameters are classified according to their roles into ecologically motivated parameters, model-scale parameters, and assumption-based parameters. Their baseline values are used as reference values for mathematical analysis and numerical simulations. Since the model has not been calibrated using field demographic time-series data, these values are not interpreted as direct empirical estimates of actual population conditions in Ujung Kulon National Park.

The proposed model is analysed in terms of positivity, boundedness, global existence and uniqueness, equilibrium points, local stability, bifurcation, numerical convergence, and normalized parameter sensitivity, using analytical derivations, Jacobian eigenvalues, numerical simulations, and relative parameter perturbations. The study focuses on the qualitative behaviour of the model rather than on estimating actual population sizes.

2.2. Mathematical Model Formulation

The dynamics of Langkap, forage vegetation, and the Javan rhinoceros are formulated as the following system of three ordinary differential equations:

$$\begin{aligned}\frac{dL}{dt} &= r_L L\left(1-\frac{L}{K_L}\right) - uL,\\ \frac{dP}{dt} &= r_P P\left(1-\frac{P}{K_P(L)}\right) - \frac{aPR}{b+P},\\ \frac{dR}{dt} &= r_R R\left(1-\frac{R}{K_R(H)}\right) + \frac{eaPR}{b+P} - \mu R.\end{aligned} \tag{1}$$

The carrying capacity of forage vegetation is assumed to depend on Langkap density and is expressed as

$$K_P(L) = \frac{K_{P0}}{1+\alpha L}, \tag{2}$$

where as the carrying capacity of the Javan rhinoceros population is assumed to decrease with increasing human pressure, as represented by

$$K_R(H) = \frac{K_{R0}}{1+\beta H}. \tag{3}$$

In system (1), Langkap growth follows logistic growth with a constant control intensity u. The influence of Langkap on forage vegetation is represented by the reduction in its effective carrying capacity through equation (2). Rhinoceros consumption of forage vegetation is described using a Holling type II functional response, which represents a saturating consumption rate as forage availability increases. This functional response is commonly used to describe nonlinear feeding interactions in predator–prey and plant–herbivore models [8-9],[11]. The parameter e represents the efficiency of converting consumed forage into rhinoceros population growth. Human pressure affects the rhinoceros population indirectly through the reduction of its effective carrying capacity, as described in equation (3). The formulation of the system follows the general structure of ecological population models involving logistic growth and nonlinear species interactions [5],[8]. The baseline parameter values and their descriptions are presented in Table 1.

2.3. Model Variables and Parameters

The state variables and parameters used in the model, together with their baseline values and roles, are presented in Table 1. The selection of state variables is based on ecological studies documenting Langkap distribution, vegetation diversity, and the conservation requirements of the Javan rhinoceros in Ujung Kulon National Park [1-3]. The model consists of three state variables: Langkap density $L(t)$ forage vegetation availability $P(t)$, and Javan rhinoceros population $R(t)$. The parameters describe the intrinsic growth rates, carrying capacities, interaction mechanisms, Langkap control intensity, and human-pressure effects.

Table 1. Variables and Parameters of the Model

Symbol	Description	Baseline	Status
$L_{(t)}$	Langkap density	–	State variable
$P_{(t)}$	Javan rhinoceros forage vegetation availability	–	State variable
$R_{(t)}$	Javan rhinoceros population	–	State variable
r_L	Intrinsic growth rate of Langkap	0.07	Baseline
K_L	Langkap carrying capacity	250	Model scale
u	Langkap control intensity	0.03	Baseline/assumption
r_P	Intrinsic growth rate of forage vegetation	0.60	Baseline/assumption
K_{P0}	Baseline carrying capacity of forage vegetation	250	Model scale
α	Coefficient of Langkap influence on forage vegetation carrying capacity	0.01	Baseline/assumption
a	Forage vegetation consumption intensity	0.15	Baseline/assumption
b	Consumption response saturation parameter	20	Baseline/assumption
rR	Intrinsic growth rate of Javan rhinoceros	0.05	Baseline/assumption
K_{R0}	Baseline carrying capacity of the Javan rhinoceros population	150	Model scale
β	Human-pressure influence coefficient	0.50	Baseline/assumption
H	Human-pressure index	0.60	Baseline/assumption
e	Forage vegetation utilization efficiency	0.10	Baseline/assumption
μ	Natural loss rate of Javan rhinoceroses	0.02	Baseline/assumption

Model-scale parameters set the scale of the carrying capacities, whereas assumption-based parameters represent the strengths of the ecological interactions. The human-pressure index H is treated as a dimensionless relative index. Thus, its baseline value should not be interpreted as an actual percentage of human pressure measured in the field. Similarly, the carrying capacity functions $K_P(L)$ and $K_R(H)$ represent simplifying mathematical assumptions concerning the effects of Langkap density and human pressure, respectively.

2.4. Mathematical Analysis

Mathematical analysis is conducted to examine the fundamental properties of system (1). The analysis covers the positivity and boundedness of solutions, global existence and uniqueness, equilibrium points, local stability, and bifurcation behaviour. These procedures follow the general framework of dynamical systems analysis [28-29].

2.4.1. Positivity of Solutions

The positivity of solutions is examined to ensure that all state variables remain nonnegative for nonnegative initial conditions. For the first equation of system (1), we obtain

$$\frac{dL}{dt} = L\left[r_L\left(1-\frac{L}{K_L}\right)-u\right]. \tag{4}$$

Similarly, the second equation can be written as

$$\frac{dP}{dt} = P\left[r_P\left(1-\frac{P}{K_P(L)}\right)-\frac{aR}{b+P}\right], \tag{5}$$

while the third equation can be written

$$\frac{dR}{dt} = R\left[r_R\left(1-\frac{R}{K_R(H)}\right)+\frac{eaP}{b+P}-\mu\right]. \tag{6}$$

Since $b+P \geq b > 0$ in the nonnegative region, the denominators in system (1) remain strictly positive. For positive initial condition, $L(0) > 0$, $P(0) > 0$, and $R(0) > 0$, each state variable can be expressed in exponential form as follows:

$$\begin{aligned} L(t) &= L(0)\exp\left\{\int_0^t\left[r_L\left(1-\frac{L(s)}{K_L}\right)-u\right]ds\right\}, \\ P(t) &= P(0)\exp\left\{\int_0^t\left[r_P\left(1-\frac{P(s)}{K_P(L(s))}\right)-\frac{aR(s)}{b+P(s)}\right]ds\right\}, \\ R(t) &= R(0)\exp\left\{\int_0^t\left[r_R\left(1-\frac{R(s)}{K_R(H)}\right)+\frac{eaP(s)}{b+P(s)}-\mu\right]ds\right\}. \end{aligned} \tag{7}$$

Since the exponential factors are strictly positive, it follows that $L(t), P(t), R(t) > 0$ as long as the solution exists. Furthermore, when $L = 0$, $P = 0$, and $R = 0$, the corresponding derivative is zero. Hence, no solution starting in the nonnegative region can cross the coordinate boundaries into the negative region. Therefore, the nonnegative region

$$\mathbb{R}^3_+ = \{(L,P,R) \in \mathbb{R}^3 : L \geq 0,\ P \geq 0,\ R \geq 0\}$$

is positively invariant. Thus, solutions with nonnegative initial conditions remain nonnegative for all times during which they exist.

2.4.2. Boundedness of Solutions

The boundedness of solutions is established by deriving an upper bound for each state variable. For the Langkap variable, equation (4) can be rewritten as

$$\frac{dL}{dt} = (r_L - u)L - \frac{r_L}{K_L}L^2. \tag{8}$$

Assuming that $0 \leq u < r_L$, the Langkap population is bounded above by

$$L(t) \leq M_L = \max\left\{L(0), K_L\left(1-\frac{u}{r_L}\right)\right\}. \tag{9}$$

Furthermore, from the carrying capacity function of forage vegetation we obtain

$$K_P(L) = \frac{K_{P0}}{1+\alpha L} \leq K_{P0}, \tag{10}$$

provided that $K_{P0} > 0, \alpha \geq 0$, and $L \geq 0$. Since the consumption term is nonnegative and $r_P > 0$, the second equation of system (1) satisfies

$$\frac{dP}{dt} \leq r_P P\left(1-\frac{P}{K_{P0}}\right). \tag{11}$$

Consequently, by the comparison principle, the forage vegetation population is bounded above by

$$P(t) \leq M_P = \max\{P(0), K_{P0}\}. \tag{12}$$

For the Javan rhinoceros population, the Holling type II functional response satisfies

$$0 \leq \frac{P}{b+P} \leq 1, \tag{13}$$

provided that $b > 0$ and $P \geq 0$. Moreover, the carrying capacity of the Javan rhinoceros population satisfies

$$K_R(H) = \frac{K_{R0}}{1+\beta H} \leq K_{R0} \tag{14}$$

for $K_{R0} > 0, \beta \geq 0$, and $H \geq 0$. Since $r_R, a, e \geq 0$, the third equation of system (1) yields

$$\frac{dR}{dt} \leq R\left[r_R - \mu + ea - \frac{r_R}{K_{R0}}R\right]. \tag{15}$$

The condition

$$r_R - \mu + ea > 0 \tag{16}$$

is required to obtain a positive upper bound for the Javan rhinoceros population. For the baseline parameter values, this condition is satisfied because

$$\begin{aligned} r_R - \mu + ea &= 0.05 - 0.02 + (0.10)(0.15) \\ &= 0.05 - 0.02 + 0.015 \\ &= 0.045 > 0. \end{aligned}$$

Hence, assuming $r_R > 0$, the comparison principle gives the following upper bound:

$$R(t) \leq M_R = \max\left\{R(0), \frac{K_{R0}(r_R - \mu + ea)}{r_R}\right\}. \tag{17}$$

Thus, the solution remains within the bounded region

$$\Omega = [0, M_L] \times [0, M_P] \times [0, M_R]. \tag{18}$$

The upper bound M_R is conservative because it is derived using K_{R0}, whereas the actual carrying capacity satisfies $K_R(H) \leq K_{R0}$. Therefore, all state variables remain bounded for nonnegative initial conditions under the specified parameter conditions.

2.4.3. Global Existence and Uniqueness of Solutions

The right-hand side of system (1) is continuous and locally Lipschitz continuous with respect to the state variables in the nonnegative region. This property follows from the differentiability of the model functions and the positivity of their denominators in that region. According to the Picard–Lindelöf theorem, for every nonnegative initial condition, system (1) admits a unique local solution [28]. Furthermore, the positivity analysis establishes that the nonnegative region is positively invariant, while the boundedness analysis shows that the solution remains within a bounded region under the specified parameter conditions. Therefore, the solution cannot exhibit finite-time blow-up. Consequently, the unique local solution can be extended for all $t \geq 0$. Thus, system (1) admits a unique global solution in the nonnegative region under the parameter conditions established in Subsections 2.4.1 and 2.4.2.

2.4.4. Equilibrium Points

The equilibrium points of system (1) are obtained by setting all derivatives equal to zero:

$$\frac{dL}{dt} = \frac{dP}{dt} = \frac{dR}{dt} = 0. \tag{19}$$

From the first equation of system (1), we obtain

$$L\left[r_L\left(1 - \frac{L}{K_L}\right) - u\right] = 0. \tag{20}$$

Therefore, the equilibrium value of Langkap is given by either

$$L^* = 0 \tag{21}$$

or

$$L^* = K_L\left(1 - \frac{u}{r_L}\right), \qquad r_L > u. \tag{22}$$

For an interior equilibrium, we consider the positive value of L^*. The corresponding carrying capacities of forage vegetation and the Javan rhinoceros population are then given by

$$K_P^* = \frac{K_{P0}}{1+\alpha L^*}, \qquad K_R^* = \frac{K_{R0}}{1+\beta H}. \tag{23}$$

To determine an interior equilibrium, we consider with $P^* > 0$ and $R^* > 0$. Setting the second equation of system (1) equal to zero and dividing by P^*, we obtain

$$r_P\left(1-\frac{P^*}{K_P^*}\right) - \frac{aR^*}{b+P^*} = 0.$$

Solving this equation for R^* gives

$$R_P(P^*) = \frac{r_{P(b+P^*)}}{a}\left(1-\frac{P^*}{K_P^*}\right), \tag{24}$$

Meanwhile, setting the third equation of system (1) equal to zero and dividing by R^*, we obtain

$$r_R\left(1-\frac{R^*}{K_R^*}\right) + \frac{eaP^*}{b+P^*} - \mu = 0.$$

Solving this equation for R^* gives

$$R_R(P^*) = \frac{K_R^*}{r_R}\left[r_R - \mu + \frac{eaP^*}{b+P^*}\right]. \tag{25}$$

Thus, the interior equilibrium is determined by finding the intersection of the two functions, namely

$$R_P(P^*) = R_R(P^*). \tag{26}$$

The admissible solution must satisfy

$$0 < P^* < K_P^*,$$

to ensure that $R^* > 0$. Once P^* has been obtained, the corresponding value of R^* can be calculated by substituting P^* into either equation (24) or equation (25).

Using the baseline parameter values listed in Table 1, the positive equilibrium value of Langkap is obtained as

$$L^* = 250\left(1-\frac{0.03}{0.07}\right) = 142.857143.$$

The corresponding carrying capacities are

$$K_P^* = \frac{250}{1+(0.01)(142.857143)} = 102.941176,$$

and

$$K_R^* = \frac{150}{1+(0.50)(0.60)} = 115.384615.$$

By numerically solving equation (26) within the admissible interval $0 < P^* < K_P^*$, the positive equilibrium values of forage vegetation and the Javan rhinoceros population are obtained as

$$P^* = 77.374532, \qquad R^* = 96.736413.$$

Therefore, the biologically meaningful interior equilibrium point of system (1) is

$$\boxed{E_7 = (142.857143,\ 77.374532,\ 96.736413).}$$

2.5. Numerical Simulation

Numerical simulations are conducted to investigate the dynamical behaviour of system (1) and examine the convergence of its solutions toward the interior equilibrium point. Four different initial conditions are considered to evaluate whether the system approaches the same equilibrium from different initial states. The numerical solutions are obtained using the ode45 solver in MATLAB, which implements an explicit Runge–Kutta method of orders 4 and 5 with adaptive step-size control

[30]. The simulations are performed over the time intervals specified for each initial condition to investigate the long-term behaviour of the system.

The resulting numerical solutions are compared with the analytically determined interior equilibrium point, $E_7 = (L^*, P^*, R^*)$. To quantitatively evaluate the convergence of the numerical solutions, the relative error of each state variable is calculated at a selected simulation time T. The maximum relative error is defined as

$$\boxed{\varepsilon_{\max}(T) = \max_{i\in\{L,P,R\}} \left\{ \frac{|x_i(T) - x_i^*|}{|x_i^*|} \times 100\% \right\}}$$

where $x_i(T)$ denotes the numerical value of the i-th state variable at time T while x_i^* denotes its corresponding equilibrium value. A smaller value of $\varepsilon_{\max}(T)$ indicates that the numerical solution is closer to the interior equilibrium point. The convergence assessment is carried out by comparing the maximum relative errors obtained from different initial conditions and selected simulation times.

2.6. Sensitivity Analysis

Sensitivity analysis is performed to measure the relative response of the positive equilibrium to changes in selected model parameters, which helps identify parameters with substantial influence on model outcomes [15–17]. The sensitivity coefficients are approximated using the central finite difference method with a relative perturbation of

$$\Delta q_j = \delta q_j, \qquad 0 < \delta < 1,. \tag{27}$$

where q_j denotes the parameter being perturbed and δ is the relative perturbation factor. The central finite difference approximation of the partial derivative of the equilibrium component x_i^* with respect to q_j is given by

$$\frac{\partial x_i^*}{\partial q_j} \approx \frac{x_i^*(q_j + \Delta q_j) - x_i^*(q_j - \Delta q_j)}{2\Delta q_j}.$$

The normalized sensitivity coefficient is then defined as

$$S_{q_j}^{x_i^*} = \frac{q_j}{x_i^*}\frac{\partial x_i^*}{\partial q_j} \approx \frac{x_i^*\left(q_j(1+\delta)\right) - x_i^*\left(q_j(1-\delta)\right)}{2\delta x_i^*}. \tag{28}$$

,

Here, x_i^* represents one component of the positive equilibrium, namely L^*, P^*, orR^*, while q_j denotes the parameter being analyzed. For each perturbation, the positive equilibrium is recalculated while the other parameters are kept fixed at their baseline values. The parameters analyzed are u, α, H, β, a, and μ. Signed coefficients indicate the direction of the equilibrium response (positive: increase; negative: decrease), whereas absolute values compare the magnitude of influence among parameters. A larger absolute coefficient indicates a stronger relative influence on the corresponding equilibrium component.

3. Results and Discussion

3.1. Model Equilibrium Points

Solving the equilibrium system by setting $\dot{L} = \dot{P} = \dot{R} = 0$ yields eight equilibrium points for the baseline parameter values, namely

$E_0 = (0,0,0)$,
$E_1 = (0,0,69.23076924)$,
$E_2 = (142.8571428,0,0)$,
$E_3 = (142.8571428,0,69.23076924)$,
$E_4 = (0,250,0)$,
$E_5 = (142.8571428,102.9411765,0)$,

$$E_6 = (0,224.1414018,101.0104706),$$
$$E_7 = (142.8571428,77.37453204,96.73641295).$$

For the baseline parameters

$$r_L = 0.07, \qquad u = 0.03, \qquad K_L = 250, \tag{29}$$

the positive equilibrium value of Langkap is obtained as

$$L^* = K_L\left(1 - \frac{u}{r_L}\right) = 250\left(1 - \frac{0.03}{0.07}\right) = 142.8571428. \tag{30}$$

The corresponding carrying capacities of forage vegetation and the Javan rhinoceros population are calculated as

$$K_P^* = \frac{250}{1 + 0.01(142.8571428)} = 102.9411765, \tag{31}$$

and

$$K_R^* = \frac{150}{1 + 0.50(0.60)} = 115.3846154. \tag{32}$$

Solving equation (26) numerically yields the positive equilibrium values

$$P^* = 77.37453204, R^* = 96.73641295. \tag{33}$$

Therefore, the interior equilibrium point is

$$\boxed{E_7 = (142.8571428,\ 77.37453204,\ 96.73641295)}. \tag{34}$$

Since $L^* > 0$, $P^* > 0$, and $R^* > 0$, the equilibrium point E_7 satisfies the positivity conditions and is therefore classified as an interior equilibrium point in the nonnegative state space.

The existence of an interior equilibrium indicates that the model allows the three populations to coexist under the baseline parameters, consistent with plant–herbivore studies in which coexistence equilibria arise when resource availability and population growth are balanced [5],[8],[31]. Langkap control affects the Langkap equilibrium directly and forage vegetation indirectly through $K_P(L)$. while the rhinoceros population depends on forage consumption and its effective carrying capacity. Accordingly, E_7 is a mathematical coexistence condition under the selected parameters rather than an estimate of the actual population sizes in Ujung Kulon National Park.

3.2. Existence and Uniqueness of the Interior Equilibrium

The existence of the interior equilibrium is analyzed by defining the function

$$F(P) = R_P(P) - R_R(P), \tag{35}$$

where $R_P(P)$ and $R_R(P)$ are given by equations (24) and (25) respectively.
The function $F(P)$ is continuous on the interval

$$0 \le P \le K_P^*, \tag{36}$$

At $P = 0$, we obtain

$$F(0) = \frac{r_P b}{a} - \frac{K_R^*(r_R - \mu)}{r_R}. \tag{37}$$

Thus, a sufficient condition for $F(0) > 0$ is

$$\frac{r_P b}{a} > \frac{K_R^*(r_R - \mu)}{r_R}. \tag{38}$$

Furthermore, at $P = K_P^*$, we have

$$R_P(K_P^*) = 0, \tag{39}$$

which gives

$$F(K_P^*) = -\frac{K_R^*}{r_R}\left[r_R - \mu + \frac{eaK_P^*}{b + K_P^*}\right]. \tag{40}$$

If

$$r_R > \mu, \tag{41}$$

then

$$F(K_P^*) < 0. \tag{42}$$

For the baseline parameters, the condition for a positive interior equilibrium is satisfied:

$$r_L > u \quad \Rightarrow \quad 0.07 > 0.03, \tag{43}$$

Moreover,

$$r_R > \mu \quad \Rightarrow \quad 0.05 > 0.02. \tag{44}$$

Furthermore, we obtain

$$\frac{r_P b}{a} = \frac{(0.60)(20)}{0.15} = 80, \tag{45}$$

whereas

$$\frac{K_R^*(r_R - \mu)}{r_R} = \frac{(115.3846154)(0.05 - 0.02)}{0.05} = 69.23076924. \tag{46}$$

Since

$$80 > 69.23076924, \tag{47}$$

It follows that

$$F(0) > 0. \tag{48}$$

Since $F(0) > 0$ and $F(K_P^*) < 0$, the Intermediate Value Theorem guarantees the existence of at least one P^* in the interval

$$0 < P^* < K_P^* \tag{49}$$

such that $F(P^*) = 0$. Hence, at least one interior equilibrium exists for the baseline parameters.
To examine the uniqueness of this equilibrium under the baseline parameters, we obtain

$$K_P^* = \frac{1750}{17}, \qquad K_R^* = \frac{1500}{13}. \tag{50}$$

Substituting these values into $R_P(P)$ gives

$$R_P(P) = -\frac{34}{875}P^2 + \frac{564}{175}P + 80, \tag{51}$$

whereas

$$R_R(P) = \frac{450(3P + 40)}{13(P + 20)}. \tag{52}$$

Equating the two functions yields

$$-\frac{34}{875}P^2 + \frac{564}{175}P + 80 = \frac{450(3P + 40)}{13(P + 20)}. \tag{53}$$

After simplification, the following polynomial equation is obtained

$$221P^3 - 13910P^2 - 230975P - 1225000 = 0. \tag{54}$$

The coefficients in equation (54) have the sign pattern

$$+, \ -, \ -, \ -, \tag{55}$$

Since there is exactly one sign change, Descartes' Rule of Signs guarantees exactly one positive real root. Combined with the existence result established previously, this implies that the positive root is the only biologically admissible solution for the forage vegetation component. Consequently, the model has exactly one interior equilibrium for the baseline parameter values. The resulting equilibrium is

$$E_7 = \big(142.857143,\ 77.374532,\ 96.736413\big).$$

The uniqueness of the interior equilibrium is important because it indicates that the proposed system has only one biologically meaningful coexistence state under the specified baseline conditions. Similar analyses of plant–herbivore and predator–prey models use equilibrium conditions to investigate the existence of coexistence states and the persistence of interacting populations [5],[8],[31]. Bešo et al. [5], for example, examined the relationship between food limitation and the existence of equilibrium

states, while Shabbir et al. [8] and Ferreira et al. [31] investigated how nonlinear interaction mechanisms influence equilibrium behaviour and bifurcation structures.

However, the uniqueness established in this study is restricted to the baseline parameter values. It does not imply that the interior equilibrium remains unique for all possible parameter combinations. Changes in Langkap control intensity, forage consumption, or human pressure may alter the equilibrium conditions and require a separate existence and uniqueness analysis. Therefore, the result should be interpreted as a baseline mathematical property rather than a general conclusion for the entire parameter space.

3.3. Local Stability and Bifurcation Analysis

The local stability of the equilibrium points is analyzed using the Jacobian matrix of system (1), given by

$$J(L,P,R) = \begin{pmatrix} r_L - u - \dfrac{2r_L L}{K_L} & 0 & 0 \\ -\dfrac{r_P \alpha P^2}{K_{P0}} & r_P - \dfrac{2r_P(1+\alpha L)P}{K_{P0}} - \dfrac{abR}{(b+P)^2} & -\dfrac{aP}{b+P} \\ 0 & \dfrac{eabR}{(b+P)^2} & r_R - \dfrac{2r_R(1+\beta H)R}{K_{R0}} + \dfrac{eaP}{b+P} - \mu \end{pmatrix}. \quad (56)$$

An equilibrium point is locally asymptotically stable if all eigenvalues of its Jacobian matrix have negative real parts. Conversely, an equilibrium point is unstable if at least one eigenvalue has a positive real part. The eigenvalues and stability classifications of the equilibrium points are presented in Table 2.

Table 2. Eigenvalue analysis and equilibrium classification

Equilibrium point	Eigenvalues	Classification
E_0	0.04, 0.60, 0.03	Repeller
E_1	−0.03, 0.04, 0.08076923	Saddle
E_2	−0.04, 0.60, 0.03	Saddle
E_3	−0.03, −0.04, 0.08076923	Saddle
E_4	−0.60, 0.04, 0.04388889	Saddle
E_5	−0.60, −0.04, 0.04255981	Saddle
E_6	−0.04393140, −0.48080252, 0.04	Saddle
E_7	−0.04317971, −0.33131236, −0.04	Locally asymptotically stable

Based on Table 2, E_0 is classified as a repeller because all its eigenvalues are positive, whereas E_1 through E_6 are saddle points due to the presence of eigenvalues with both positive and negative signs. In contrast, the interior equilibrium $E_7 = 142.857143, 77.374532, 96.736413$, has three negative eigenvalues, namely $-0.04317971, -0.33131236,$ and -0.04. Therefore, E_7 is locally asymptotically stable. This indicates that sufficiently small perturbations around the interior equilibrium decay over time, allowing the system to return to its equilibrium state. These stability characteristics are consistent with the general theory of continuous dynamical systems, in which the signs of the real parts of Jacobian eigenvalues determine the local behaviour of hyperbolic equilibrium points [28-29]. The results indicate that the coexistence equilibrium can be locally stable even when several boundary equilibria are unstable or saddle points.

To further investigate the stability changes, a bifurcation analysis is performed by considering the Langkap control rate (u) as the bifurcation parameter, while the other parameters are fixed at their baseline values. From the first equation of system (1), the equilibrium branches for Langkap are $L_1^* = 0$ and $L_2^* = K_L\left(1 - \frac{u}{r_L}\right)$ These branches coincide at the critical value $u_c = r_L = 0.07$. The eigenvalue associated with the Langkap component at the boundary equilibrium is $\lambda_L = r_L - u$. Thus, this eigenvalue becomes zero at $u = 0.07$. At the critical value, the boundary equilibrium and the positive Langkap equilibrium branch coincide in the full three-dimensional system. The corresponding equilibrium is $E_c = (0,\ 224.141402,\ 101.010471)$. The other two eigenvalues at this point remain negative:

$$\lambda_2 = -0.48080252, \qquad \lambda_3 = -0.04393140.$$

Furthermore, the Langkap equation satisfies the nondegeneracy conditions for a transcritical bifurcation because $\frac{\partial^2 f_L}{\partial L \partial u} \neq 0$ and $\frac{\partial^2 f_L}{\partial L^2} \neq 0$. The numerical results around the critical value are summarized in Table 3.

Table 3. Bifurcation analysis with respect to the Langkap control rate (u)

u	Equilibrium branch	L^*	λ_L	Stability
0.030	Positive	142.857	−0.040	Stable
0.030	Boundary	0	+0.040	Saddle
0.069	Positive	3.571	−0.001	Stable
0.069	Boundary	0	+0.001	Saddle
0.070	Branch intersection	0	0	Non-hyperbolic
0.071	Boundary	0	−0.001	Stable

The results indicate an exchange of stability between the positive and boundary equilibrium branches at $u = 0.07$, characterizing a transcritical bifurcation. This finding is consistent with ecological bifurcation theory, in which changes in a control or growth parameter can alter the stability of boundary equilibria and the persistence of interacting populations [5],[8],[31]. Bešo et al. [5] also demonstrated that transcritical bifurcations can occur at parameter thresholds associated with population persistence in plant–herbivore systems.

From an ecological perspective, the critical value $u_c = 0.07$ represents a mathematical threshold at which the positive Langkap equilibrium reaches zero. For $u < u_c$, the positive Langkap equilibrium is biologically admissible, whereas for $u > u_c$, the positive branch produces a negative Langkap value and is therefore biologically inadmissible. This threshold provides a theoretical description of the relationship between Langkap control intensity and its persistence within the proposed model. It should not, however, be interpreted as a direct operational control recommendation without parameter calibration using field data.

3.4. Numerical Simulation and Convergence

Numerical simulations are performed using four different initial conditions, as summarized in Table 4, to examine whether the solutions converge toward the interior equilibrium. The simulation results show that all four trajectories approach the interior equilibrium, as illustrated in Figures 2–5.

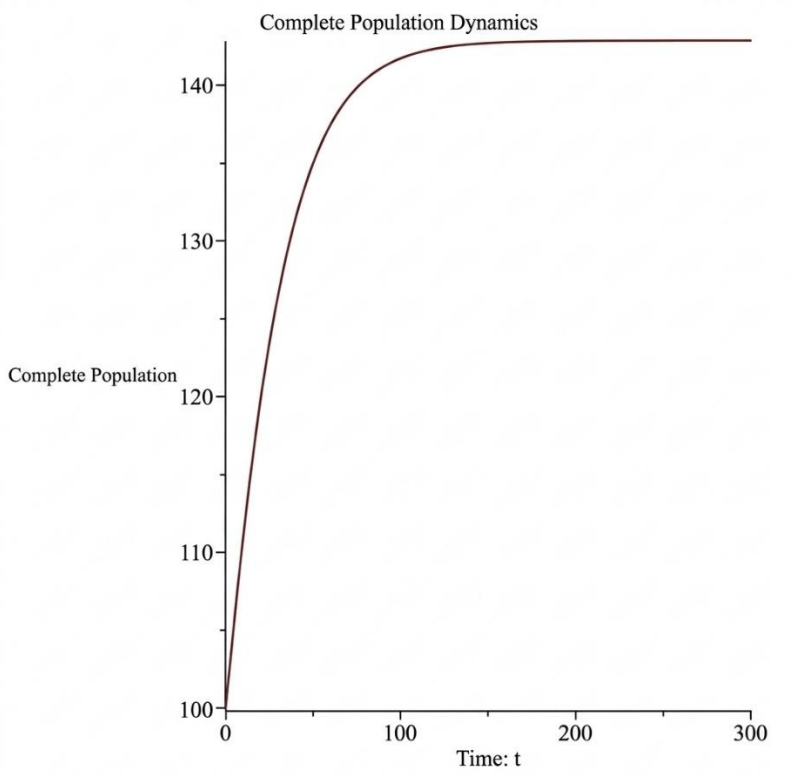


Figure 2. Langkap Simulation

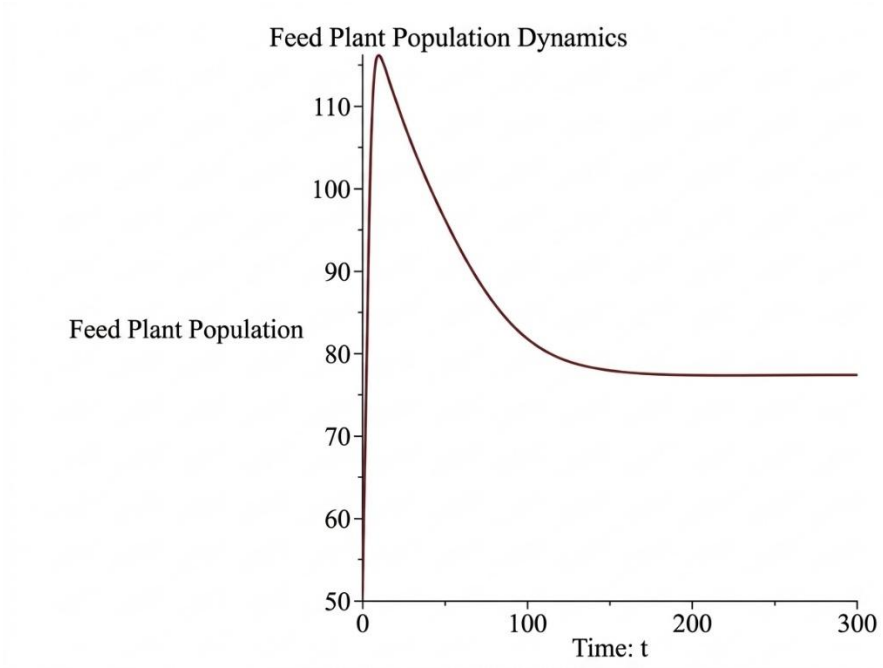


Figure 3. Forage Vegetaion Simulation

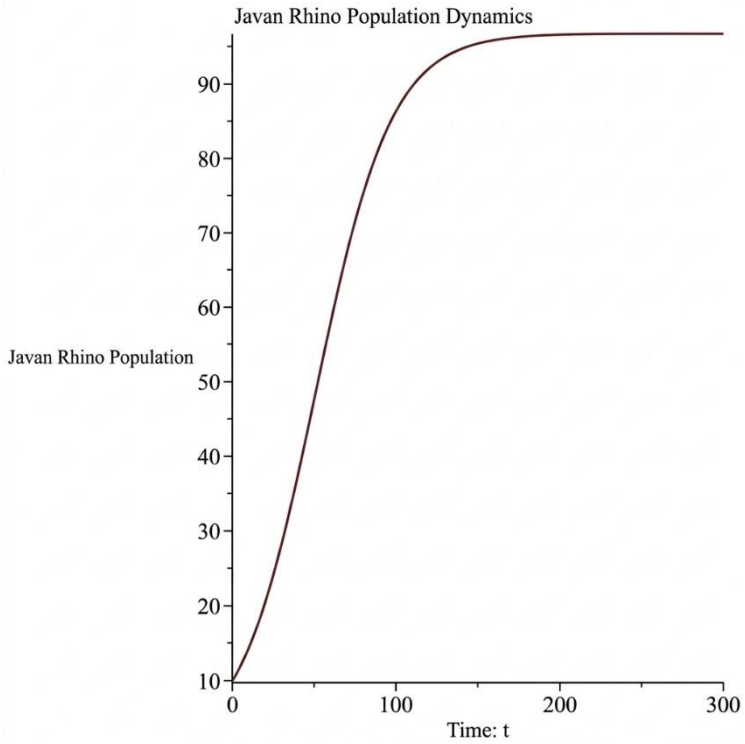


Figure 4. Rhino Simulation

For the initial condition

$$(L(0), P(0), R(0)) = (100,50,10), \tag{57}$$

The numerical solution at $t = 300$, is

$$(L, P, R) = (142.8567669,\ 77.3755259,\ 96.7344539), \tag{58}$$

While at $t = 500$, it becomes

$$(L, P, R) = (142.8571427,\ 77.3745423,\ 96.7364125). \tag{59}$$

For the other three initial conditions, the numerical solutions also approach E_7 at $t = 1000$. The numerical convergence results are presented in Table 4. Numerical simulation results and maximum relative error with respect to E_7.

Table 4. Numerical convergence from different initial conditions

Initial condition	t	L(t)	P(t)	R(t)	Maximum relative error
(100,50,10)	300	142.8567669	77.3755259	96.7344539	2.03×10^{-5}
(100,50,10)	500	142.8571427	77.3745423	96.7364125	1.33×10^{-7}
(150,70,20)	1000	142.8571429	77.3745319	96.7364129	1.81×10^{-9}
(200,30,5)	1000	142.8571429	77.3745260	96.7364130	7.81×10^{-8}
(50,90,15)	1000	142.8571429	77.3745429	96.7364128	1.40×10^{-7}

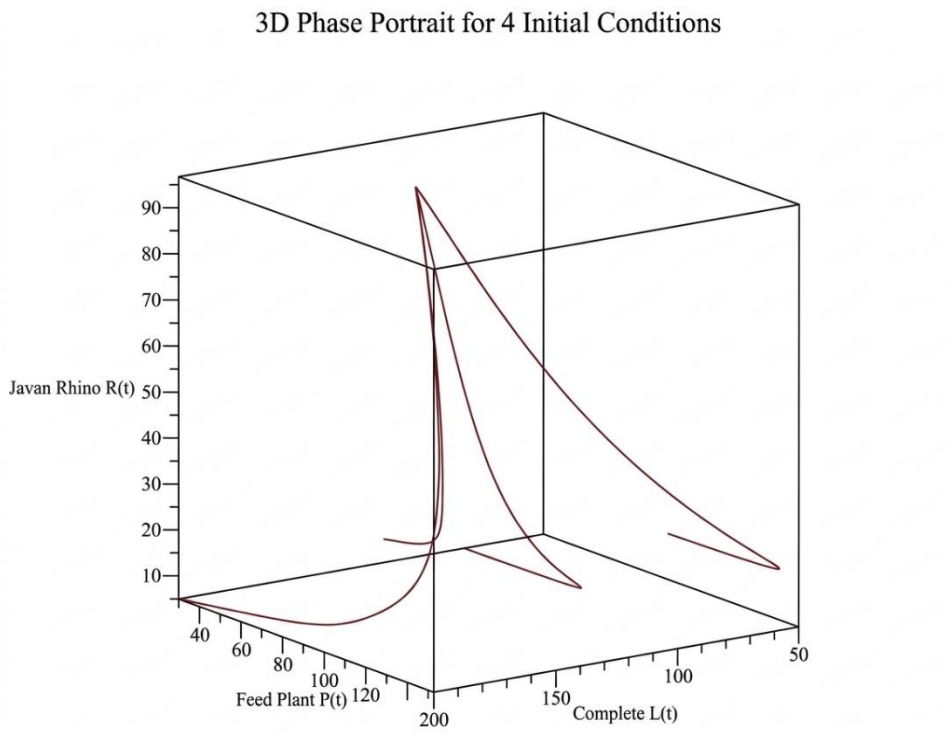


Figure 5. Three-Dimensional Numerical Phase Portrait

The numerical results show that the maximum relative error decreases to a small value for all tested initial conditions. For the initial condition $(100,50,10)$, the maximum relative error decreases from 2.03×10^{-5} at $t = 300$ to 1.33×10^{-7} at $t = 500$. Similarly, the other initial conditions produce maximum relative errors below 10^{-7} at 10^{-7}, indicating that the numerical solutions are close to the calculated interior equilibrium.

This numerical behaviour is consistent with the local asymptotic stability established through the Jacobian eigenvalue analysis. In continuous dynamical systems, negative real parts of all eigenvalues indicate that sufficiently small perturbations around a hyperbolic equilibrium decay over time [29-30]. Comparable relationships between analytical stability results and numerical trajectories have also been examined in plant–herbivore and predator–prey models [5],[8],[28]. The convergence observed from the four initial conditions provides additional numerical evidence supporting the local stability of E_7. However, convergence from a finite number of initial conditions does not establish global asymptotic stability. Furthermore, the attempted Lyapunov approach does not provide sufficient conditions to establish global stability for the proposed system. Therefore, the global stability of E_7 remains an open question for further investigation.

3.5. Parameter Sensitivity Analysis

Sensitivity analysis is conducted to examine the influence of selected model parameters on the positive equilibrium state. The parameters considered are u, α, H, β, a, and μ, with a relative perturbation of 1%. The normalized sensitivity coefficients are calculated using the central finite difference method described in Equation (27) and (28). This analysis helps identify the parameters that have the greatest influence on the equilibrium state and provides insight into the sensitivity of ecological model outcomes to parameter variations [15-16]. Similar approaches have been used to examine parameter uncertainty in ecological models involving forest biomass and wildlife populations [17]. The sensitivity analysis results for the positive equilibrium state are presented in Table 5

Table 5. Sensitivity Indices

Parameter	L^*	P^*	R^*
u	-0.750000	0.583010	0.034047
α	0	-0.777358	-0.045407
H	0	0.100766	-0.224886
β	0	0.100766	-0.224886
a	0	-0.560845	0.251576
μ	0	0.208330	-0.464943

For the Langkap variable, the parameter u has the largest absolute sensitivity. This result can also be derived analytically from the equilibrium equation

$$L^* = K_L\left(1 - \frac{u}{r_L}\right). \tag{60}$$

The normalized sensitivity coefficient with respect to u is

$$S_u^{L^*} = -\frac{u}{r_L - u}. \tag{61}$$

Using the baseline parameters $u = 0.03$ and $r_L = 0.07$, we obtain

$$S_u^{L^*} = -\frac{0.03}{0.07 - 0.03} = -0.75. \tag{62}$$

This negative value indicates that a relative increase in the Langkap control parameter u is associated with a relative decrease in the equilibrium value of L^*. For forage vegetation, the parameter α has the largest absolute sensitivity, with

$$\left|S_\alpha^{P^*}\right| = -0.777358. \tag{63}$$

This indicates that, under the baseline scenario, a relative change in the parameter representing the effect of Langkap on forage vegetation carrying capacity produces the largest relative response in P^* among the parameters considered. The consumption parameter a has negative sensitivity with respect to P^* and positive sensitivity with respect to R^*. These results indicate that an increase in consumption intensity is associated with a decrease in the equilibrium forage vegetation level, while the contribution of consumption to Javan rhinoceros growth through the term $\frac{eaPR}{b+P}$ is associated with an increase in the equilibrium rhinoceros population. For the Javan rhinoceros population, the parameter μ has the largest absolute sensitivity under the baseline scenario, namely

$$\left|S_\mu^{R^*}\right| = -0.464943. \tag{64}$$

The parameter a also gives a relative response in R^* of

$$\left|S_a^{R^*}\right| = 0.251576, \tag{65}$$

While the sensitivity to the human-pressure index is

$$\left|S_H^{R^*}\right| = -0.224886. \tag{66}$$

The negative value of $S_H^{R^*}$ indicates that an increase in the human-pressure index is associated with a decrease in the equilibrium value of the Javan rhinoceros population within the model structure. These results suggest that natural mortality has the greatest local influence on the rhinoceros equilibrium, followed by consumption intensity and human pressure.The sensitivity coefficients with respect to H and β are identical because both parameters enter the model through the product βH in the carrying capacity function

$$K_R(H) = \frac{K_{R0}}{1 + \beta H}. \quad (67)$$

To further examine this relationship, define the combined parameter $\tilde{H} = \beta H$. The rhinoceros carrying capacity can therefore be expressed as $K_{R(\tilde{H})} = \frac{K_{R0}}{1+\tilde{H}}$. Consequently, the equilibrium values depend on H and β through the combined parameter $\tilde{H}$, rather than on each parameter independently. The normalized sensitivity coefficient with respect to $\tilde{H}$ is therefore equal to the sensitivity coefficients with respect to H and β, such that

$$\boxed{S_{\tilde{H}}^{(x^*)} = S_H^{(x^*)} = S_\beta^{(x^*)}, \quad x^* \in \{L^*, P^*, R^*\}} \quad (68)$$

This relationship indicates a structural identifiability limitation: the individual effects of H and β cannot be distinguished independently based solely on the equilibrium structure of this model. Only their combined effect through $\tilde{H}$ can be assessed. Thus, estimating H and β separately would require additional information or independent data. These limitation should also be considered when interpreting sensitivity results, since parameter uncertainty and model structure may affect the conclusions drawn from ecological models [15-16]. Overall, the sensitivity results represent local mathematical sensitivities around the baseline parameter values. Therefore, these values should not be directly interpreted as empirical causal relationships in the field without calibration and validation using ecological data.

3.6. Scenario Analysis and Ecological Interpretation

Scenario analysis is conducted by varying the Langkap control parameter and human-pressure index independently while keeping the remaining parameters at their baseline values. The analysis is intended to examine how changes in these two parameters affect the interior equilibrium of the proposed system.

Table 6. Equilibrium values under different Langkap control scenarios

u	L^*	P^*	R^*
0.01	214.2857	54.2206	94.5184
0.03	142.8571	77.3745	96.7364
0.05	71.4286	120.0943	98.9044

As shown in Table 6, increasing Langkap control intensity from $u = 0.01$ to $u = 0.05$ reduces the Langkap equilibrium density from 214.2857 to 71.4286. In contrast, forage vegetation availability increases from 54.2206 to 120.0943. The rhinoceros equilibrium population also increases from 94.5184 to 98.9044, corresponding to an increase of approximately 4.64%.

These results indicate that increasing Langkap control can indirectly support the rhinoceros population within the proposed model. The mechanism occurs through the reduction of Langkap density, which increases the effective carrying capacity of forage vegetation. The increase in forage availability subsequently provides greater resources for the rhinoceros population. This relationship is consistent with the ecological concept that invasive vegetation can alter plant community composition and resource availability. Studies of Langkap distribution and vegetation diversity in Ujung Kulon provide the ecological context for examining this interaction [1],[3]. Furthermore, research on Javan rhinoceros conservation emphasizes the importance of maintaining suitable habitat conditions and food resources for population persistence [2].

Table 7. Equilibrium values under different human pressure scenarios

H	L^*	P^*	R^*
0.30	142.8571	72.6927	108.9483
0.60	142.8571	77.3745	96.7364
0.90	142.8571	80.7283	86.9414

Table 7 shows that increasing human pressure from $H = 0.30$ to $H = 0.90$ decreases the rhinoceros equilibrium population from 108.9483 to 86.9414, corresponding to a reduction of approximately 20.20%. This decline occurs because increasing human pressure reduces the effective carrying capacity of the rhinoceros population through the function $K_R(H) = \frac{K_{R0}}{1+\beta H}$.

Interestingly, forage vegetation availability increases from 72.6927 to 80.7283 as human pressure increases, due to the decline in the rhinoceros population and the resulting reduction in forage consumption. However, this increase does not necessarily indicate improved ecosystem conditions, as it occurs alongside a decline in the rhinoceros population. This finding highlights the potential impact of human pressure on wildlife populations and habitat conditions [25-27], as well as the importance of considering ecological consequences in invasive-species management strategies [20],[23-24]. Overall, increasing Langkap control improves forage availability and slightly increases the equilibrium population of Javan rhinoceros, whereas increasing human pressure reduces the rhinoceros population. These findings indicate the importance of balancing invasive-plant control with habitat protection.

4. Conclusion

Based on the analysis of the Langkap–forage vegetation–Javan rhinoceros dynamical model, several conclusions can be drawn. The proposed model describes the interactions among Langkap growth, forage vegetation availability, and Javan rhinoceros population dynamics by incorporating Langkap control and human pressure through density- and pressure-dependent carrying capacities. For the baseline parameters, the system has eight equilibrium points: seven boundary equilibria and one interior equilibrium

$$E_7 = (142.8571428,\ 77.37453204,\ 96.73641295). \quad (69)$$

Its existence is established by the Intermediate Value Theorem and its uniqueness by Descartes' Rule of Signs, but this uniqueness is restricted to the baseline parameter set.

The stability analysis indicates that E_0 is an unstable repeller, whereas E_1 through E_6 are saddle points. At the interior equilibrium E_7, all three eigenvalues have negative real parts, confirming its local asymptotic stability. Numerical simulations from four different initial conditions also show convergence toward E_7. However, these numerical results only demonstrate convergence for the tested initial conditions and do not establish global stability.

The sensitivity analysis (1% perturbation) shows that u has the largest absolute sensitivity for L^*, α for P^*, and μ for R^*, followed by a and H. The identical coefficients for H and β arise because both enter the model only through βH, so their effects cannot be separated by this model structure alone. The baseline parameters are modelling assumptions that have not been calibrated against empirical data; the findings are therefore mathematical results under the specified model structure. Future research should focus on parameter estimation from field observations, empirical validation, and additional ecological factors.

References

[1] Siswoyo, S., Muntasib, E. K. S. H., & Haryanto, D. (2024). Study of plant diversity in the Javan Rhino Study and Conservation Area (JRSCA), Ujung Kulon National Park. *Media Konservasi, 29*(2), 288–293.

[2] Wilson, S. G., Biggs, D., & Kark, S. (2022). Protecting an icon: Javan rhinoceros frontline management and conservation. *Oryx,* 56(1), 101–107.

[3] Damarjati, S., Nugraha, W. A., & Arjasakusuma, S. (2022). Mapping the invasive palm species Arenga obtusifolia using multiple endmember spectral mixture analysis (MESMA) and PRISMA hyperspectral data in Ujung Kulon National Park, Indonesia. Geocarto International, 37(27), 18254–18274.

[4] Koch, F., Tietjen, B., Tielbörger, K., & Allhoff, K. T. (2023). Livestock management promotes bush encroachment in savanna systems by altering plant–herbivore feedback. Oikos, 2023(3), e09462.

[5] Bešo, E., Kalabušić, S., & Pilav, E. (2024). Food-limited plant–herbivore model: Bifurcations, persistence, and stability. *Mathematical Biosciences, 370*, 109157.

[6] Hamada, M. Y. (2024). Dynamical analysis of a discrete-time plant–herbivore model. *Arabian Journal of Mathematics,* 13, 121–131.

[7] Alsubhi, M., Ahmed, R., Alraddadi, I., Alsharif, F., & Imran, M. (2024). Stability and bifurcation analysis of a discrete-time plant-herbivore model with harvesting effect. *AIMS Mathematics,* 9(8), 20014–20042.

[8] Shabbir, M. S., Din, Q., De la Sen, M., & Gómez-Aguilar, J. F. (2024). Exploring dynamics of plant–herbivore interactions: bifurcation analysis and chaos control with Holling type-II functional response. *Journal of Mathematical Biology*, 88(1), 8.

[9] Stollenwerk, N., Aguiar, M., & Kooi, B. W. (2022). Modelling Holling type II functional response in deterministic and stochastic food chain models with mass conservation. *Ecological Complexity*, 49, 100982.

[10] Ramesh, K., Ranjith Kumar, G., & Nisar, K. S. (2023). A nonlinear mathematical model on the dynamical study of a fractional-order delayed predator–prey scheme that incorporates harvesting together and Holling type-II functional response. *Results in Applied Mathematics,* 19, 100390.

[11] Arias, C. F., Blé, G., & Falconi, M. (2022). Dynamics of a discrete-time predator–prey system with Holling II functional response. *Qualitative Theory of Dynamical Systems,* 21, 31.

[12] Ruan, M., & Li, X. (2024). Complex dynamical properties and chaos control for a discrete modified Leslie-Gower prey-predator system with Holling II functional response. *Advances in Continuous and Discrete Models,* 2024, 30.

[13] Wyse, S. K., Martignoni, M. M., Mata, M. A., Foxall, E., & Tyson, R. C. (2022). Structural sensitivity in the functional responses of predator–prey models. *Ecological Complexity,* 51, 101014.

[14] Kuiper, J. J., Kooi, B. W., Peterson, G. D., & Mooij, W. M. (2022). Bridging theories for ecosystem stability through structural sensitivity analysis of ecological models in equilibrium. *Acta Biotheoretica,* 70, 18.

[15] Lusardi, L., André, E., Castañeda, I., Lemler, S., Lafitte, P., Zarzoso-Lacoste, D., & Bonnaud, E. (2024). Methods for comparing theoretical models parameterized with field data using biological criteria and Sobol analysis. *Ecological Modelling,* 493, 110728.

[16] Luján, C., Shin, Y.-J., Barrier, N., Leadley, P., & Oliveros-Ramos, R. (2025). A protocol for implementing parameter sensitivity analyses in complex ecosystem models. *Ecological Modelling,* 501, 110990.

[17] Fanuel, I. M., Mirau, S., Kajunguri, D., & Moyo, F. (2023). Conservation of forest biomass and forest-dependent wildlife population: Uncertainty quantification of the model parameters. *Heliyon,* 9(6), e16948.
[18] Marangi, C., Martiradonna, A., & Ragni, S. (2023). Optimal resource allocation for spatiotemporal control of invasive species. *Applied Mathematics and Computation,* 439, 127614.
[19] Di Liddo, A., & Martiradonna, A. (2025). Effective management of invasive alien species in an optimal control framework. *Decisions in Economics and Finance,* 48, 1837–1868.
[20] Pascual, A., Giardina, C. P., Povak, N. A., Hessburg, P. F., Heider, C., Salminen, E., & Asner, G. P. (2022). Optimizing invasive species management using mathematical programming to support stewardship of water and carbon-based ecosystem services. *Journal of Environmental Management,* 301, 113803.
[21] Das, D., Kar, T. K., & Pal, D. (2023). The impact of invasive species on some ecological services in a harvested predator–prey system. *Mathematics and Computers in Simulation,* 212, 66–90.
[22] Lee, S., Han, C. Y., Kim, M., & Kang, Y. (2022). Optimal control of a discrete-time plant–herbivore/pest model with bistability in fluctuating environments. *Mathematical Biosciences and Engineering,* 19(5), 5075–5103.
[23] Waring, T. K., Somers, V. L. J., McCarthy, M. A., & Baker, C. M. (2024). When to monitor or control: Informed invasive species management using a partially observable Markov decision process (POMDP) framework. *Methods in Ecology and Evolution,* 15(9), 1667–1676.
[24] Baker, C. M., Blonda, P., Casella, F., Diele, F., Marangi, C., Martiradonna, A., et al. (2023). Using remote sensing data within an optimal spatiotemporal model for invasive plant management: the case of Ailanthus altissima in the Alta Murgia National Park. *Scientific Reports,* 13, 14587.
[25] Gaynor, K. M., et al. (2025). The influence of human presence and footprint on animal space use in US national parks. *Proceedings of the Royal Society B,* 292(2051), 20251013.
[26] Hertel, A. G., Parres, A., Frank, S. C., et al. (2025). Human footprint and forest disturbance reduce space use of brown bears (Ursus arctos) across Europe. *Global Change Biology,* 31(1), e70011.
[27] DuPuy, P., Galaitsi, S., & Linkov, I. (2025). Carrying capacity in human-environment interactions: a systematic review. *Integrated Environmental Assessment and Management,* 21(3), 526–539.
[28] Seifert, C., Trostorff, S., & Waurick, M. (2022). *Evolutionary equations: Picard's theorem for partial differential equations, and applications* (Vol. 287). Cham: Birkhäuser.
[29] Strogatz, S. H. (2024). *Nonlinear dynamics and chaos: with applications to physics, biology, chemistry, and engineering*. CRC press.
[30] Mathworks. (2022). Solve Nonstiff Differential Equations–Medium Order Method-MATLAB Ode45.
[31] Ferreira, J. D., Molina, W. L., Perez, J. J., & González, A. P. (2025). Stability and bifurcation analysis in predator-prey system involving Holling type-II functional response. *Mathematical Biosciences and Engineering,* 22(10), 2559–2594.